

## Entanglement Interferometry for Precision Measurement of Atomic Scattering Properties

Artur Widera,<sup>1,2,\*</sup> Olaf Mandel,<sup>1,2</sup> Markus Greiner,<sup>3</sup> Susanne Kreim,<sup>1,2</sup>  
Theodor W. Hänsch,<sup>1,2</sup> and Immanuel Bloch<sup>1,2,4</sup>

<sup>1</sup>Ludwig-Maximilians-Universität, Schellingstrasse 4/III, 80799 Munich, Germany

<sup>2</sup>Max-Planck-Institut für Quantenoptik, 85748 Garching, Germany

<sup>3</sup>JILA, University of Colorado, Boulder, Colorado 80309-0440, USA

<sup>4</sup>Johannes-Gutenberg-Universität, Staudingerweg 7, 55128 Mainz, Germany

(Received 30 October 2003; published 23 April 2004)

We report on a matter wave interferometer realized with entangled pairs of trapped <sup>87</sup>Rb atoms. Each pair of atoms is confined at a single site of an optical lattice potential. The interferometer is realized by first creating a coherent spin superposition of the two atoms and then tuning the interstate scattering length via a Feshbach resonance. The selective change of the interstate scattering length leads to an entanglement dynamics of the two-particle state that can be detected in a Ramsey interference experiment. This entanglement dynamics is employed for a precision measurement of atomic interaction parameters. Furthermore, the interferometer allows us to separate lattice sites with one or two atoms in a nondestructive way.

DOI: 10.1103/PhysRevLett.92.160406

PACS numbers: 03.75.Gg, 03.75.Lm, 03.75.Mn, 34.50.-s

The controlled creation of entanglement is one of the most subtle and challenging tasks in modern quantum mechanics, with both wide reaching practical and fundamental implications. In neutral atom based systems, significant progress has been made during recent years in the generation of large spin-squeezed samples of atomic gases [1] or the controlled creation of Greenberger-Horne-Zeilinger (GHZ) states [2] in cavity QED systems [3]. In addition, it has been recognized early on that in binary spin superpositions of Bose-Einstein condensed quantum gases (with spin states  $|0\rangle$  and  $|1\rangle$ ) a large amount of entanglement could be created by controlling the difference in interaction strengths  $\chi = 1/2(U_{00} + U_{11} - 2U_{01})$  between the particles in different spin states [4–8]. Here,  $U_{ij}$  denotes the interaction matrix element between atoms in spin states  $i$  and  $j$ . Such control can either be achieved by moving atoms on different sites in spin-dependent optical lattice potentials [5,8–11] or by tuning the scattering lengths, such that  $\chi \neq 0$  [4,7,12]. In the latter case, the simple creation of a coherent spin superposition, e.g., by an initial  $\pi/2$  pulse, followed by a subsequent evolution of the spin system, would automatically lead to highly spin-squeezed or entangled  $N$ -particle GHZ-like states. Here we demonstrate such entanglement dynamics with pairs of atoms trapped in the ground state of a potential well in an optical lattice. Such pairs form a unique and highly controllable model system to study interactions between two particles. By using a recently predicted interstate Feshbach resonance in <sup>87</sup>Rb [13], we are able to control  $\chi$  and thus accelerate the ensuing entanglement evolution, so that it is observable in a Ramsey type experiment within our coherence time. We show that this dynamical evolution of the atom pairs into entangled and disentangled states can be used to obtain precise information on the scattering properties of the systems. The entangle-

ment interferometer makes it furthermore possible to separate singly occupied lattice sites from doubly occupied sites in a nondestructive way.

The Ramsey interferometer sequence used in the experiment consists of two  $\pi/2$  pulses that couple the two states  $|0\rangle \equiv |F=1, m_F=+1\rangle$  and  $|1\rangle \equiv |F=2, m_F=-1\rangle$ . Here,  $F$  and  $m_F$  denote the total angular momentum and its projection, respectively. The pulse separation is  $t_{\text{hold}}$  and the phase  $\alpha$  of the last pulse can be varied. Between the two  $\pi/2$  pulses, the interaction behavior  $\chi$  of the atoms is modified by using a Feshbach resonance occurring between atoms in hyperfine states  $|0\rangle$  and  $|1\rangle$  [13,14]. In the case of a single isolated atom, initially in the state  $\psi_1^i = |0\rangle$ , the effect of a changing interaction behavior has no consequence for the particle since it does not interact with other particles. After applying the experimental sequence shown in Fig. 1, the final state reads  $\psi_1^f = 1/2(b_+|0\rangle - b_-|1\rangle)$  with  $b_{\pm} \equiv 1 \pm e^{\mp i\alpha}$ . The probability of finding the atom in state  $|1\rangle$  is simply given by  $P_1^f(\alpha) = \frac{1}{2}(1 - \cos\alpha)$ , which describes the usual Ramsey fringes without decoherence.

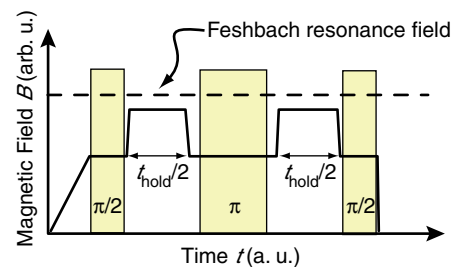


FIG. 1 (color online). Ramsey interferometer sequence (shaded bars). Ramsey fringes are obtained by varying the phase  $\alpha$  of the last microwave  $\pi/2$  pulse. The magnetic field can be ramped to different magnetic field values in order to change the interaction properties of the atoms.

In the case of two particles, the change of interaction parameters leads to an additional entangling-disentangling dynamics which is markedly different. Let us consider two bosonic atoms in the internal state  $\psi_2^i = |0\rangle \otimes |0\rangle \equiv |00\rangle$ . First, a  $\pi/2$  pulse places the atoms in a coherent superposition of the two internal states  $\psi_2 = \frac{1}{2}(|00\rangle - |01\rangle - |10\rangle + |11\rangle)$ . After a time  $t$ , each two-particle state obtains a phase factor  $e^{-i\phi_{ij}}$  due to interactions, where  $\phi_{ij} = (U_{ij}/\hbar)t_{\text{hold}}$  is the collisional phase shift, with  $U_{ij} = (4\pi\hbar^2 a_{ij})/m \times \int d^3x |\varphi_i|^2 |\varphi_j|^2$  being the on-site interaction matrix element. Here,  $a_{ij}$  represents the elastic scattering length between particles in states  $i$  and  $j$ ,  $\varphi_{i(j)}$  is the ground state wave function of an atom in spin state  $i(j)$ , and  $m$  the mass of a single atom. For  $t = t_{\text{hold}}/2$ , the two-particle state then evolves into  $\psi_2 = \frac{1}{2}(e^{-i(\phi_{00}/2)}|00\rangle - e^{-i(\phi_{01}/2)}|01\rangle - e^{-i(\phi_{10}/2)}|10\rangle + e^{-i(\phi_{11}/2)}|11\rangle)$ , where  $\phi_{01} = \phi_{10}$ . After a spin echo  $\pi$  pulse, a further interaction time  $t_{\text{hold}}/2$  and a last  $\pi/2$  pulse, the final state reads  $\psi_2^f = \frac{1}{2}\{c_c^+|00\rangle - c_s(|01\rangle + |10\rangle) + c_c^-|11\rangle\}$ , where  $c_c^\pm \equiv e^{\mp i\alpha}(\cos\alpha \pm e^{-i\phi_\chi})$ ,  $c_s \equiv i\sin\alpha$ , and  $\phi_\chi \equiv -(\phi_{00} + \phi_{11} - 2\phi_{01})/2$ . The probability of finding an atom in state  $|1\rangle$  can then be expressed by  $P_2^f(\alpha, \phi_\chi) = \frac{1}{2}(1 - \cos\alpha \cos\phi_\chi)$ , which is modulated in amplitude compared to the case of single atoms.

Four main cases illustrate the dynamics of the two-particle system. (i) For  $\phi_\chi = 0$  the Ramsey fringe  $P_2^f(\alpha, \phi_\chi = 0) = \frac{1}{2}(1 - \cos\alpha)$  is identical to the fringe of an isolated particle as shown above. (ii) If the interactions lead to a phase difference of  $\phi_\chi = \pi/2$ , the final state  $\psi_2^f(\phi_\chi = \pi/2)$  is a maximally entangled Bell-like state. For such a state, the corresponding Ramsey fringe  $P_2^f(\alpha, \phi_\chi = \pi/2) = \frac{1}{2}$  does not exhibit any modulation [11]. (iii) When the phase difference is increased to  $\phi_\chi = \pi$ , the system is disentangled again, and the corresponding Ramsey fringe  $P_2^f(\alpha, \phi_\chi = \pi) = \frac{1}{2}(1 + \cos\alpha)$  is phase shifted by  $\pi$  with respect to the case of a single particle. It should be noted that for this interaction phase the state vectors of isolated atoms and atoms being part of an atom pair are orthogonal to each other. Therefore, by choosing a specific single particle phase, either isolated atoms or atom pairs can be transferred into the  $|F = 2\rangle$  state and removed by a subsequent resonant laser pulse. The remaining atoms would form a pure lattice of either single atoms or atom pairs, which again can evolve to Bell-like pairs. For even larger phase differences, the system entangles and disentangles again, until for (iv)  $\phi_\chi = 2\pi$  the system exhibits a Ramsey fringe which is in phase with the fringe of a single atom. In a system containing  $N_1$  isolated single atoms and  $N_2/2$  isolated pairs of atoms, the total fringe will be a weighted sum of the two distinct fringes and will have a visibility according to:

$$V(\chi) = V_0 e^{-(t/\tau_1)} \{(1 - n_2) + n_2 e^{-(t/\tau_2)} \cos\phi_\chi\}, \quad (1)$$

where we have included decoherence and two-body losses with time constants  $\tau_1$  and  $\tau_2$ , respectively,  $V_0$  is a finite

initial visibility [15] and  $n_i = N_i/(N_1 + N_2)$ ,  $i = 1, 2$  with  $n_1 + n_2 = 1$ . Whereas the contribution of isolated atoms to the fringe visibility  $V$  remains unaffected under a change of  $\chi$ , the total fringe signal shows a dynamics with the same periodicity as  $P_2^f$ . In the following, we consider the experimentally relevant case  $N_1 > N_2$ . For zero phase difference  $\phi_\chi = 0$ , we expect to measure a Ramsey fringe with high visibility  $V$ . The visibility decreases for increasing  $\phi_\chi$  and reaches a minimum for  $\phi_\chi = \pi$  where the fringes from single atoms and from atom pairs are out of phase and partially compensate each other in the total signal. For larger interaction phase differences, the total visibility increases, until it shows a maximum for  $\phi_\chi = 2\pi$ , where the two Ramsey fringes are completely in phase again. It should be noted that the interaction time  $t_R$  after which  $\phi_\chi = 2\pi$  depends on the difference in the interaction matrix elements  $U_{ij}$ , and for constant overlap of the wave functions on the elastic scattering length difference  $\Delta a_{s,\chi} \equiv -\frac{1}{2}(a_{00} + a_{11} - 2a_{01})$ .

The experimental setup is similar to our previous work [16,17]. We start with a BEC of up to  $3 \times 10^5$   $^{87}\text{Rb}$  atoms trapped in the hyperfine ground state  $|F = 1, m_F = -1\rangle$ . We load the BEC into a pure two- or three-dimensional optical lattice potential formed by three mutually orthogonal standing waves of far detuned light. For the three-dimensional case, the system undergoes a Mott-insulator transition [16,18] with one and two atoms per site. The wavelengths used for the different standing waves are 829 nm ( $y$  and  $z$  axis) and 853 nm ( $x$  direction), with trapping frequencies at each lattice site of  $\omega_x = 2\pi \times 33$ ,  $\omega_y = 2\pi \times 43$ , and  $\omega_z = 2\pi \times 41$  kHz. In order to preserve spin polarization of the atoms in the optical trap, we maintain a 1 G magnetic offset field along the  $x$  direction. The atoms are prepared in the Feshbach resonance sensitive spin superposition by transferring the population from the  $|F = 1, m_F = -1\rangle$  state into the  $|0\rangle \equiv |F = 1, m_F = +1\rangle$  hyperfine level via a radio frequency (rf) Landau-Zener sweep. We then increase the magnetic field to 8.63 G. By applying a microwave field around 6.8 GHz and rf radiation around 6 MHz, we are able to coherently couple the two internal states  $|0\rangle$  and  $|1\rangle$  with a two-photon transition similar to [19].

In order to locate the position of the Feshbach resonance through enhanced atomic losses, we load the BEC into a two-dimensional ( $x$  and  $y$  axis) optical lattice potential. The atomic density is thereby strongly increased compared to a simple dipole trap, thus loss processes occur with higher probability. The magnetic field is subsequently increased to different values within 10  $\mu\text{s}$ . After holding the atoms for 1 ms at a specific magnetic field, we switch off all trapping potentials and magnetic fields to measure the remaining total atom number in a time-of-flight (TOF) measurement (see Fig. 2). The magnetic field has been calibrated by measuring the frequency of the  $|F = 1, m_F = -1\rangle \rightarrow |F = 2, m_F = -2\rangle$  microwave transition at different magnetic field values and employing the Breit-Rabi formula to determine the

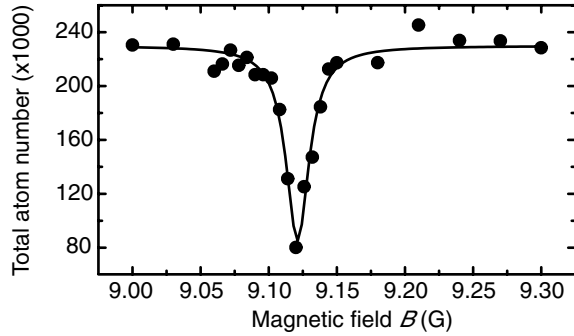


FIG. 2. Measurement of total atom number versus magnetic field in a 2D optical lattice. The solid line is a Lorentzian fit to the data with center at 9.121(9) G and a width of 20(5) mG. The hold time at the various magnetic field values is 1 ms.

actual field strength. Because of background magnetic field fluctuations, the magnetic field calibration has an uncertainty of 3 mG, noise of the magnetic field creating current source introduces an uncertainty of 2 mG and an additional systematic error of 4 mG is added by the optical trapping potential. The measured position of 9.121(9) G of the resonance agrees well with the predicted value of 9.123 G within our measurement uncertainty [20]. In order to determine the ratio of single to paired atoms in our three-dimensional lattice potential, we monitor the loss of atoms when we hold the atomic sample at the resonance magnetic field for a variable time (see Fig. 3).

Lattice sites which are occupied by more than one atom are depleted within 3 ms due to the increased two-body collision rates and the high density at single lattice sites. Isolated atoms, however, are protected from collisions and remain trapped. Assuming a negligible number of sites with three atoms, a fit with an exponential decay yields a time constant of 1.3(2) ms and a ratio  $N_1/N_2 \approx 1.1$ .

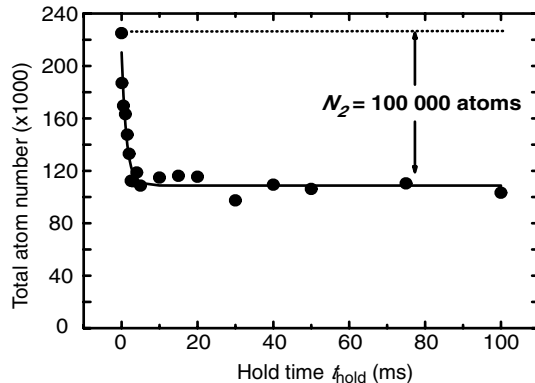


FIG. 3. Time resolved measurement of the total atom number at the measured Feshbach resonance in a 3D lattice potential. Sites with more than one atom are emptied within 3 ms, whereas sites with only one atom are protected from loss. The solid line is a fit to an exponential decay with offset, from which we find to have a ratio  $N_1/N_2 \approx 1.1$ .

In order to determine the elastic scattering properties, we apply the Ramsey interferometer sequence that has been described earlier (see Fig. 1). At each magnetic field value, we record the Ramsey fringe visibility for different interaction times  $t_{\text{hold}}$  (see, e.g., Fig. 4 for a field of  $B = 9.081$  G).

The revival time  $t_R$  at which the visibility shows its maximum is determined by a fit using Eq. (1). This revival time depends on the difference in the interaction matrix element. A single revival of the fringe visibility could in principle also be caused by a complete loss of lattice sites with two atoms. We have, however, checked that even for the more pronounced losses at the Feshbach resonance the system exhibits dynamics due to interaction after the first revival. In this case, losses would shift the revival time by a few percent.

In order to extract information on the changes in the scattering length from the revival times, one can measure the on-site matrix element  $U_{00}$  through a collapse and revival experiment that we have demonstrated earlier [17]. For the same experimental parameters, we find  $U_{00} = h/396(11) \mu\text{s}$ . Using this information we can calculate  $\chi/U_{00} = \Delta a_{s,\chi}/a_{00}$ , which expresses the change in scattering length measured in units of the scattering length  $a_{00}$ . In order to map out the change in the elastic scattering length on the Feshbach resonance,  $\Delta a_{s,\chi}/a_{00}$  has been measured for several magnetic fields and is shown in Fig. 5. Since the entanglement interferometer can only measure absolute values of  $\Delta a_{s,\chi}/a_{00}$ , we perform a usual time of flight measurement to obtain information on the sign of the scattering length differences. For this, we leave the Feshbach field switched on for the first 3 ms of the TOF [21]. During this time, the altered interaction energy is converted into kinetic energy, and the size of the atom cloud is measured. For magnetic fields

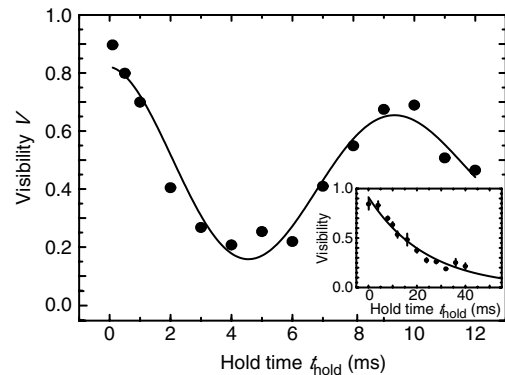


FIG. 4. Measured visibility dynamics due to entanglement in the system for a magnetic field value of 9.081 G. The solid line is a fit using Eq. (1) yielding a revival time  $t_R = 2\pi t_{\text{hold}}/\phi_\chi = 9.5(2)$  ms,  $V_0 = 0.82(4)$ ,  $n_2 = 0.5$ ,  $\tau_1 = 41(13)$  ms, and  $\tau_2 = 20(5)$  ms. The inset is a measurement of the Ramsey sequence for a constant magnetic field  $B = 8.63$  G, away from the Feshbach resonance, and the solid line is a fit describing an exponential decay of the fringe visibility.

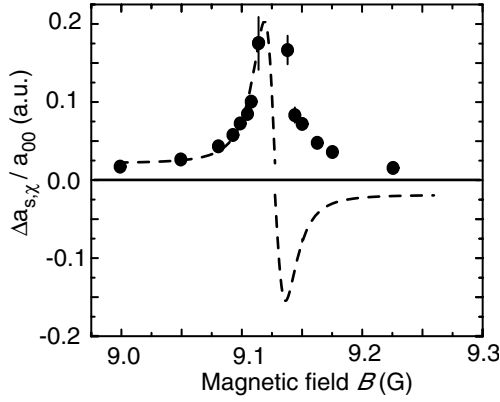


FIG. 5. Measured absolute value of the change of elastic scattering length for magnetic field values around the Feshbach resonance (dots). Both sides were fitted separately to a dispersive curve with a common center [9.128(9) G] and width [15(4) mG]. In order to illustrate the dispersive behavior of  $\Delta a_{s,\chi}$  (dashed line), the fitted branch above the resonance is flipped to negative values according to the sign determined by the TOF measurement.

below the Feshbach resonance, we have found the cloud to be slightly larger (9% change in size) in the axial direction, whereas it is slightly smaller above the Feshbach resonance. From this, we conclude that the interspecies scattering length grows and shrinks below and above the Feshbach resonance field, respectively.

Since we ramp the magnetic field through the resonance in order to address the region above the resonance, atoms acquire a small collisional phase before the hold time starts. This is why we fit both branches of the scattering length change separately to a dispersive profile, with the constraint of a common center and width. The fit yields a center of 9.128(9) G and a width of 15(4) mG, in good agreement with our loss measurements. The two branches show an offset from  $\Delta a_{s,\chi} = 0$ , because even far away from the Feshbach resonance, the different scattering lengths  $a_{ij}$  do not compensate to  $\chi = 0$ . The difference in sign of the offsets below and above the resonance is artificial, since our measurement is insensitive to the sign of  $\Delta a_{s,\chi}$ , which has been obtained through the TOF measurement.

The interferometric method presented allows for high precision measurements of relative changes of the scattering lengths. In order to demonstrate this, we assume an error-free scattering length  $a_{00} = 100.4 a_0$  [22], where  $a_0$  is the Bohr radius. With this, we determine the change of elastic scattering length for  $B = 9.081$  G to be  $\Delta a_{s,\chi} = 4.2(1) a_0$ .

In conclusion, we have presented a novel interferometric method to create and investigate entanglement dynamics in an array of spin superpositions of neutral atoms. The observed entanglement oscillations allow the precise determination of interaction properties between atoms in different spin states. We have demonstrated the

versatility of the interferometer by characterizing the elastic scattering properties of a recently predicted weak interstate Feshbach resonance in  $^{87}\text{Rb}$ . We have found both the elastic and inelastic channel of the measured Feshbach resonance to be in good agreement with the theoretical prediction. The two-particle interferometer furthermore enables the direct creation of arrays of Bell states, together with the nondestructive separation of singly from doubly occupied sites.

We would like to thank Dieter Jaksch and Servaas Kokkelmans for useful discussions, Anton Scheich for support with the electronics, and Tim Rom and Thorsten Best for assistance with the experiment. We also acknowledge financial support from the Bayerische Forschungsförderung and AFOSR.

\*Electronic address: widera@uni-mainz.de

- [1] B. Julsgaard, A. Kozhokin, and E. S. Polzik, *Nature (London)* **413**, 400 (2001).
- [2] D. M. Greenberger, M. A. Horne, A. Shimony, and A. Zeilinger, *Am. J. Phys.* **58**, 1131 (1990).
- [3] A. Rauschenbeutel *et al.*, *Science* **288**, 2024 (2000).
- [4] A. Sørensen, L.-M. Duan, J. I. Cirac, and P. Zoller, *Nature (London)* **409**, 63 (2001).
- [5] D. Jaksch, H.-J. Briegel, J. I. Cirac, C. W. Gardiner, and P. Zoller, *Phys. Rev. Lett.* **82**, 1975 (1999).
- [6] K. Helmerson and L. You, *Phys. Rev. Lett.* **87**, 170402 (2001).
- [7] L. You, *Phys. Rev. Lett.* **90**, 030402 (2003).
- [8] A. Sørensen and K. Mølmer, *Phys. Rev. Lett.* **83**, 2274 (1999).
- [9] G. K. Brennen, C. M. Caves, P. S. Jessen, and I. H. Deutsch, *Phys. Rev. Lett.* **82**, 1060 (1999).
- [10] O. Mandel *et al.*, *Phys. Rev. Lett.* **91**, 010407 (2003).
- [11] O. Mandel *et al.*, *Nature (London)* **425**, 937 (2003).
- [12] A. Micheli, D. Jaksch, J. I. Cirac, and P. Zoller, *Phys. Rev. A* **67**, 013607 (2003).
- [13] E. van Kempen, S. Kokkelmans, D. J. Heinzen, and B. J. Verhaar, *Phys. Rev. Lett.* **88**, 093201 (2002).
- [14] M. Erhard, H. Schmaljohann, J. Kronjäger, K. Bongs, and K. Sengstock, *cond-mat/0309318*.
- [15] Here the visibility is defined as  $V = (P_{\max}^{\text{tot}} - P_{\min}^{\text{tot}}) / (P_{\max}^{\text{tot}} + P_{\min}^{\text{tot}})$ .
- [16] M. Greiner *et al.*, *Nature (London)* **415**, 39 (2002).
- [17] M. Greiner *et al.*, *Nature (London)* **419**, 51 (2002).
- [18] D. Jaksch, C. Bruder, J. I. Cirac, C. W. Gardiner, and P. Zoller, *Phys. Rev. Lett.* **81**, 3108 (1998).
- [19] D. S. Hall, M. R. Matthews, J. R. Ensher, C. E. Wieman, and E. A. Cornell, *Phys. Rev. Lett.* **81**, 1539 (1998).
- [20] The interstate Feshbach resonance has recently also been detected through atom loss measurements by Erhard *et al.* [14]. There the resonance was found to be located at a magnetic field of 9.08(1) G.
- [21] S. Inouye, M. R. Andrews, J. Stenger, H.-J. Miesner, D. M. Stamper-Kurn, and W. Ketterle, *Nature (London)* **392**, 151 (1998).
- [22] S. Kokkelmans (private communication).